Coherent-feedback quantum control with a dynamic compensator

Hideo Mabuchi*
Physical Measurement and Control, Edward L. Ginzton Laboratory, Stanford University, 316 Via Pueblo Mall, Stanford, California 94305, USA

(Received 13 March 2008; revised manuscript received 2 September 2008; published 19 September 2008)

I present an experimental realization of a coherent-feedback control system that was recently proposed for testing basic principles of linear quantum stochastic control theory [M. R. James, H. I. Nurdin, and I. R. Petersen, e-print arXiv:quant-ph/0703150v2, IEEE Transactions on Automatic Control (to be published)]. For a dynamical plant consisting of an optical ring resonator, I demonstrate ~7 dB broadband disturbance rejection of injected laser signals via all-optical feedback with a tailored dynamic compensator. Comparison of the results with a transfer function model pinpoints critical parameters that determine the coherent-feedback control system's performance.

DOI: 10.1103/PhysRevA.78.032323 PACS number(s): 42.50.Ex, 02.30.Yy, 07.07.Tw

The need for versatile methodology to control quantum dynamics arises in many areas of science and technology [1]. For example, quantum dynamical phenomena are central to quantum information processing, magnetic resonance imaging and protein structure determination, atomic clocks, SQUID sensors, and many important chemical reactions. Substantial progress has been made over the past two decades in the development of intuitive approaches within specific application areas [2,3] but the formulation of an integrated, first-principles discipline of quantum control—as a proper extension of classical control theory—remains a broad priority.

It is natural to distinguish among three modes of quantum control: *open loop*, in which a quantum system is driven by a time-dependent control Hamiltonian in a predetermined way; *measurement feedback*, in which discrete or continuous measurements of some output channel of an open quantum system are used to adjust the control actions in real time; and *coherent feedback*, in which a quantized field scattered by the quantum system of interest is processed coherently (without measurement) and then redirected into the system in order to effect control. The first two modes are entirely analogous with classical open-loop and real-time feedback control, and their relation to existing engineering theory is now well understood [1]. The possibility of coherent feedback, however, gives rise to a genuinely new category of control-theoretic problems as it encompasses noncommutative signals and quantum-dynamical transformations thereof [8]. While some intriguing proposals can be found in the physics literature [9,10], relatively little is yet known about the systematic control theory of coherent feedback [12].

This paper describes an experimental implementation of coherent-feedback quantum control with optical resonators as the dynamical systems and laser beams as the coherent disturbance and feedback signals. It is presented in the context of recent developments in control theory [13–15], which have shown that optimal and robust design of quantum coherent-feedback loops can be accomplished (in certain settings) using sophisticated methods of systems engineering. As discussed by James *et al.* in their seminal paper [13], quantum coherent-feedback theory generalizes the classical theory of stochastic control by incorporating "signals" represented by quantum fields with noncommuting quadratures. My setup parallels the quantum-optical example analyzed in Sec. VII of their paper, with numerical parameters modified to facilitate experimental implementation. James *et al.* have shown that many canonical results of classical stochastic control can be generalized to the quantum setting by exploiting formal analogies between the usual Itô stochastic differential equations and quantum stochastic differential equations (QSDE's) that arise in quantum field theory in a Markovian limit [16]; the most immediate and familiar experimental setting in which QSDE's are used for practical modeling is quantum optics, and the work reported here realizes the connection between experimental practice and the theoretical advances of James *et al.* From the perspective of quantum information science, the results presented here likewise represent a first step towards the goal of developing embedded, autonomous controllers that can implement feedback-stabilization protocols without ever bringing signals up to a classical, macroscopic level.

Figure 1 presents a schematic overview of the apparatus and the coherent feedback loop. Two optical ring resonators represent the "plant" and "controller" dynamical systems; the control-theoretic design goal is to tailor the properties of the controller so as to minimize the optical power detected at output z when a "noise" signal (optical coherent state with arbitrary time-dependent complex amplitude) is injected at the input w. The component y of the noise beam that reflects from the plant input coupler is treated as the error signal, which is coherently processed by the controller to produce a feedback signal u. As discussed in [13], the controller should properly transform both quadrature amplitudes of y to produce appropriate quadrature amplitudes in u. The latter signal is fed back into the plant resonator via the output coupler, matched spatially to the same resonant mode driven by the noise input w.

While this type of coherent-feedback loop is properly described using quantum stochastic differential equations (as in [13]), a simplified analysis can be performed using Laplace transfer functions as familiar from classical linear control theory [17]. This simplification here corresponds to the stan-

*hmabuchi@stanford.edu

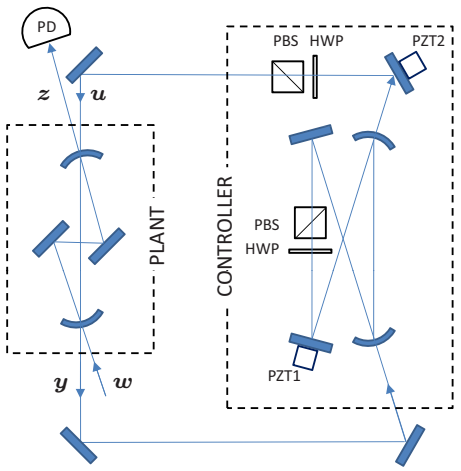

FIG. 1. (Color online) Experimental schematic showing the coupled plant and controller resonators, variable attenuators PBS HWP, piezoelectric transducers (PZT), and photodetector (PD).

dard practice of tracking only the mean values of quantum observables, which is appropriate as long as all Hamiltonians are linear and all input states are Gaussian. Following [13] we exploit the basic insight that in coherent feedback one can effectively ignore the fact that we have noncommuting signal components in the loop and manipulate Laplace transfer functions that apply simultaneously to both quadrature amplitudes of the optical fields. The open-loop (without feedback) transfer function of the plant resonator from the input w to the output z can be written $G_{zw}=-2\sqrt{k_1k_4}/(s+\gamma_p)$, where γ_p is the total plant decay rate, k_1 and k_4 are the partial rates associated with transmission through the input and output couplers, and s is the Laplace transform variable shifted to have value zero at the plant resonance frequency. In terms of physical parameters $\gamma_p=c(t_1^2+t_2^2+t_3^2+t_4^2+l^2)/4\pi L_p$, where c is the speed of light, L_p is the round-trip cavity length, t_i^2 is the power transmission coefficient of the ith mirror, and l^2 represents all other intracavity losses. When the feedback loop is implemented as shown in Fig. 1 with a controller having transfer function K_{uy}, the overall (closed-loop) transfer function from w to z becomes

$$\mathcal{S}(G,K)=G_{zw}+G_{zu}(1-K_{uy}G_{yu})^{-1}K_{uy}G_{yw}, \tag{1}$$

where the additional transfer functions are given for our setup by $G_{yu}=G_{zw}$, $G_{zu}=1-2k_4/(s+\gamma_p)$, and $G_{yw}=1-2k_1/(s+\gamma_p)$.

The *disturbance rejection* problem can now be defined as that of designing the controller so as to minimize the magnitude of $\mathcal{S}(G,K)$. This corresponds to tailoring the coherent-feedback loop in such a way as to minimize the ratio of the optical power in the output z to that of the noise input w. If we are interested in broadband disturbance rejection, it is important to note that $\mathcal{S}(G,K)$ cannot be made much smaller than G_{zw} for all values of s if K_{uy} is independent of s. Thus a simple proportional controller (for which K_{uy} is a complex number) will not suffice; we require a dynamic compensator with a nontrivial frequency response.

If we assume that our controller is itself an optical resonator, and with some foresight parametrize K_{uy} as

$$K_{uy}=\frac{2\sqrt{\eta_K}\sqrt{k_1k_4}}{s+\gamma_p-2(k_1+k_4)+\eta_\gamma}, \tag{2}$$

it follows that $\mathcal{S}(G,K)\to 0$ for all s as $\eta_\gamma\to 0$ and $\eta_K\to 1$. Under these ideal conditions, zero optical power would be observed by a perfect photodetector monitoring the output z, for any coherent optical noise signal (mode-matched laser beam with arbitrary time-varying complex amplitude) injected at the input w. In practice it is difficult to implement the ideal controller transfer function exactly, and there is an additional challenge of perfecting the spatial mode matching from the controller output to the u input of the plant cavity. In modeling the experiment I thus include a factor μ to account for imperfect spatial mode matching, η_K to represent deviation of the magnitude of K_{uy} from its ideal value, and η_γ to represent deviation of the controller decay rate from its ideal value of $\gamma_p-2k_1-2k_4$. Writing $\mathcal{S}_\mu(G,K)$ to denote the inclusion of a mode-matching correction, the ratio of the optical power in z in the closed-loop case to the open-loop case is then

$$\left|\frac{\mathcal{S}_\mu(G,K)}{G_{zw}}\right|^2=|1\pm\sqrt{\mu}S_m|^2+(1-\mu)|S_u|^2, \tag{3}$$

(with $+$ for negative and $-$ for positive coherent feedback) where

$$S_m=G_{zw}^{-1}G_{zu}(1-\sqrt{\mu}K_{uy}G_{yu})^{-1}K_{uy}G_{yw},$$

$$S_u=G_{zw}^{-1}K_{uy}G_{yw}.$$

With reference to Fig. 1, note that the resonance frequency of the controller cavity is adjustable via the actuator PZT1 and that the phase of K_{uy} is continuously variable via PZT2. In practice these must both be set appropriately in order to minimize the magnitude of $\mathcal{S}_\mu(G,K)$.

In my experiment the plant cavity is a four-mirror folded ring resonator (as depicted in Fig. 1) with measured values $\gamma_p\approx 9.3$ MHz and $L_p\approx 14.1$ cm. The controller is a four-mirror ring resonator with measured decay rate $\gamma_c\approx 7.3$ MHz and length $L_c\approx 48.6$ cm. The controller decay rate can be adjusted using the intracavity variable attenuator shown in Fig. 1. The injected signal at w, and thus the coherent-feedback loop signals y, u, and z, derive from an 852 nm diode laser. The photodetector monitoring the output signal z is placed behind an 852 nm optical-bandpass filter. Additional laser beams from an 894 nm diode laser are injected into both cavities in order to match the controller resonance frequency with that of the plant. The carrier frequency of the 894 nm laser is locked to the plant cavity resonance (which is allowed to drift freely); PZT1 is then used to lock the controller cavity resonance to an electro-optic sideband of the 894 nm laser that can be tuned over a frequency range greater than the controller cavity free spectral range. Using this arrangement it is straightforward to servocontrol the controller cavity length so that its resonance frequency coincides with that of the plant cavity for the 852 nm signal beams.

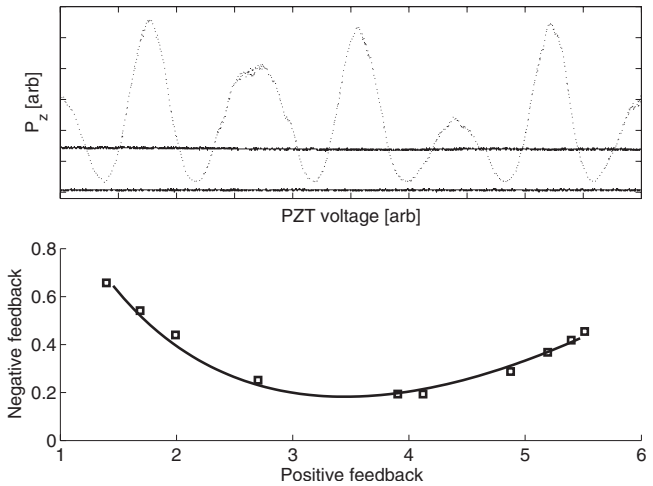

FIG. 2. Upper: variation of the total optical power in output z as PZT2 is scanned to change the coherent-feedback phase (note that several periods of the triangle-wave voltage ramp are included, with evident turning points). Lower: parametric plot of the $s=0$ closed-loop system response under positive (x coordinate) and negative (y coordinate) feedback with gain mismatch η_K ranging between approximately 0.06 and 2.2; see the text for an explanation of the theoretical curve.

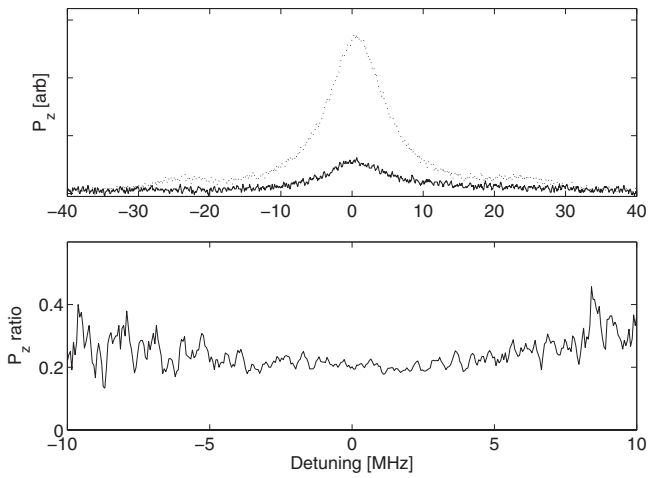

FIG. 3. Upper: optical power in z as a function of detuning between the input laser frequency and the plant resonance, corresponding to swept sine measurements of $|G_{zw}|^2$ (dashed) and $|\mathcal{S}_\mu(G,K)|^2$ (solid). Shoulders on the resonance peak are electro-optic sidebands that were added to establish the frequency scale. Lower: ratio of traces from the upper plot, confirming the broadband nature of the disturbance rejection.

Disturbance rejection via coherent feedback is demonstrated in Fig. 2. In order to generate this data the 852 nm laser is servocontrolled to track the resonance frequency of the plant cavity, thus ensuring that we initially probe all transfer functions with $s=0$. In the upper subplot, the two solid traces show the electronic noise floor (lower) and the optical power level detected at the photodetector (PD) monitoring the output z in the absence of coherent feedback (upper). When the coherent-feedback loop is closed, the optical power in z is seen to depend strongly on the coherent feedback phase as set by PZT2. If the voltage on PZT2 is ramped in order to vary the phase continuously the coherent-feedback loop oscillates between positive and negative feedback (dashed trace). The ratio of the minimum value of the optical power in z, obtained with negative coherent feedback, to the open-loop value yields an optimal disturbance rejection of approximately 7 dB. As the overall system is linear, the input power of w is unimportant and drops out of the analysis; values in the range of ~ 100 μW were used in this experiment.

The lower subplot of Fig. 2 presents a parametric plot of the maximum (horizontal axis) versus minimum (vertical axis) optical power ratios observed with η_K ranging over a set of values between 0.06 and 2.2 (adjusted using the variable attenuator at the output of the controller cavity). The curve shows the prediction obtained from the transfer-function model described above, where the values of η_γ, μ, k_1, and k_4 were adjusted within reasonable ranges to obtain a good fit to the data. The values obtained in this way are $\eta_\gamma = \eta_p/14$, $\mu=0.84$, and $t_1^2=t_4^2=0.002$. These values for the plant input- and output-coupler power transmission coefficients agree with witness sample measurements from the mirror coating run when adjusted for the beam incidence angle of 0.3 radians. The mode-matching factor μ is in agreement with a direct measurement $\mu \lesssim 0.85$ obtained by observing the ratio of TEM00 to transverse-mode transmission peaks, and η_γ agrees with the measurements of γ_p and γ_c when t_1^2 and t_4^2 are set to 0.002. This comparison of data with the transfer-function model thus confirms that the parameters affecting system performance are well known; it follows from Eq. (3) that the $s=0$ disturbance rejection performance is fundamentally limited by imperfect mode matching $\mu<1$. The model also shows that for low-frequency noise (small detuning), a small error η_γ in the controller decay rate can be overcome by adjusting η_K. But a high degree of broadband disturbance rejection (for noise inputs with frequency spread comparable to γ_p) is not possible unless η_γ is carefully minimized.

The upper subplot of Fig. 3 displays data corresponding to (single shot) swept-sine transfer function measurements of G_{zw} (dashed) and $\mathcal{S}_\mu$ (G,K) under negative coherent feedback (solid). These were obtained simply by scanning the 852 nm laser frequency over the plant cavity resonance and recording the optical power in z. The ratio of the two traces is shown in the lower subplot, which shows that suppression is achieved over a wide range of noise signal frequencies and thus establishes the broadband nature of the disturbance rejection. As the PD measures total optical power of z and the observed suppression is independent of the phase of the coherent amplitude of w, coherent feedback is here seen to operate simultaneously on both quadrature amplitudes of the noise signal.

Finally, Fig. 4 shows that it is possible to stabilize the path length of the coherent signal loop to maintain negative feedback. In order to obtain a suitable error signal an electrooptic modulator (EOM) is inserted in the y signal path as shown in the top diagram. This EOM is driven by a high-frequency (~ 1 MHz) sine wave; the signal from a photodetector (PD2) at an auxiliary output port of the plant cavity is demodulated at this frequency to produce the error signal.

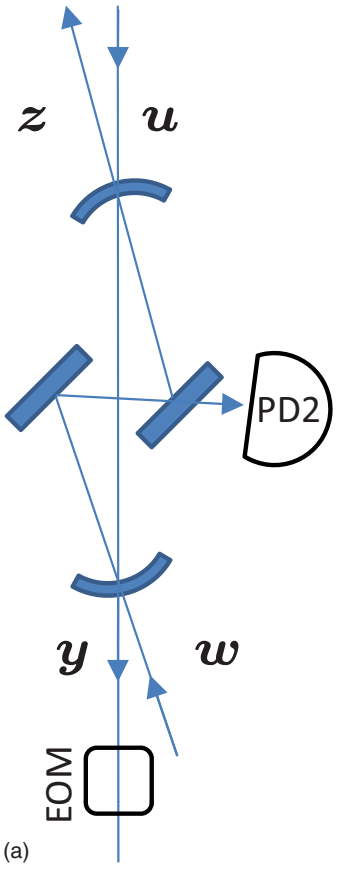

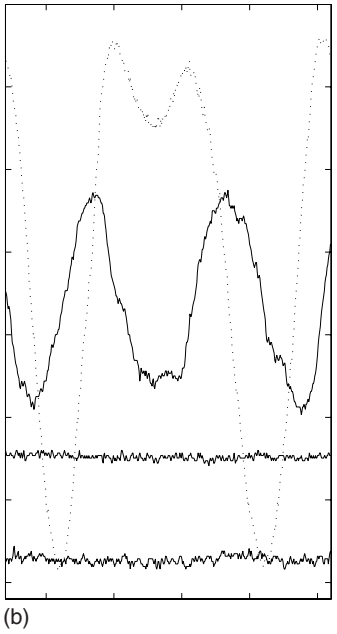

FIG. 4. (Color online) (a) schematic detail of the plant indicating additional photodetector (PD2) and electro-optic modulator (EOM) used to generate an error signal for locking the coherent-feedback phase. (b) oscillating traces depict the optical power variation of output z (dashed) and the coherent-feedback phase error signal (solid) as a function of coherent-feedback phase. The flat traces indicate the levels of optical power observed in output z with no feedback (upper) and with the phase locked to the negative feedback condition (lower).

On the bottom of Fig. 4, the oscillating traces depict the variation of the closed-loop output power in z (dashed) and the error signal (solid) as the length of the feedback loop is varied using PZT2. The minimum of the closed-loop output power is seen to coincide with a zero crossing of the error signal, thus making it possible to stabilize the coherent-feedback phase via electronic feedback to PZT2. The open-loop and phase-stabilized closed-loop optical output powers in z (with the 852 nm laser locked to the plant cavity resonance) are indicated by the flat traces in the plot.

While the experiment presented here has dealt only with coherent optical states, the coherent-feedback disturbance rejection scheme should function without significant modification for a very broad class of quantum noise signals. Existing theory based on quantum stochastic differential equations provides a rigorous basis for predicting the performance expected for squeezed-state inputs, and indeed the type of dynamic compensation demonstrated here is already of interest for tailoring spectral properties of squeezed light for applications such as gravity-wave detection [18]. From an experimental perspective it would be most interesting to test the performance with non-Gaussian quantum states such as those produced by photon subtraction [19], which would push beyond the reach of current theory.

Even within the restricted scenario of Gaussian states, it may also be noted that the coherent-feedback approach to optical disturbance rejection should be capable of achieving arbitrarily low power in the noise output z for an arbitrary optical input power at w. In contrast, it seems intuitively clear that any measurement-based feedback loop (in which the results of broadband measurements on y are used to synthesize optical states injected at u) that is capable of suppressing coherent-state noise inputs with arbitrary nonstationary magnitude and phase should exhibit a disturbance rejection noise floor such that there would be a minimum optical output power at z even for vanishing power at w. This would stem from the fact that the complex amplitude of a coherent state noise input can never be measured perfectly (in the "single-shot" sense relevant to this type of real-time feedback). For example, even an ideal balanced heterodyne photoreceiver produces electronic photocurrent noise in the absence of any real optical signal, whose fluctuations are indistinguishable in any given time interval from the photocurrent that would be produced by a very weak flux of photons appearing at the signal port. These vacuum photocurrent fluctuations would necessarily result in some sort of stochastic low-level optical feedback to the control input u, and therefore to output power at z, even in the complete absence of any noise power at w. It clearly should be possible to design a rigorous experiment that would demonstrate the superiority of coherent feedback as compared to measurement-based feedback in this setting, but this would appear to require a fairly extensive quantitative analysis as well as some experimental improvements to the stability of the apparatus.

This work was supported by the Air Force Office of Scientific Research under Grant No. FA9550-07-1-0198.

[1] H. Mabuchi and N. Khaneja, Int. J. Robust Nonlinear Control **15**, 647 (2005).

[2] V. P. Belavkin, Autom. Remote Control (Engl. Transl.) **44**, 178 (1983); A. P. Peirce, M. A. Dahleh, and H. Rabitz, Phys. Rev. A **37**, 4950 (1988); G. M. Huang, T. J. Tarn, and J. W. Clark, J. Math. Phys. **24**, 2608 (1983).

[3] H. M. Wiseman and G. J. Milburn, Phys. Rev. A **47**, 642 (1993); C. Ahn, A. C. Doherty, and A. J. Landahl, *ibid.* **65**, 042301 (2002); N. Khaneja, S. J. Glaser, and R. W. Brockett, *ibid.* **65**, 032301 (2002); A. N. Korotkov, Phys. Rev. B **60**, 5737 (1999).

[4] R. Lang and K. Kobayashi, IEEE J. Quantum Electron. **QE-16**, 347 (1980).

[5] R. Clavero, F. Ramos, and J. Martí, IEEE J. Lightwave Technol. **25**, 3641 (2007).

[6] B. Gütlich *et al.*, Appl. Phys. B: Lasers Opt. **81**, 927 (2005); M. A. Vorontsov, M. Zhao, and D. Z. Anderson, Opt. Commun. **134**, 191 (1997).

[7] Y. Liu *et al.*, IEEE Trans. Circuits Syst., I: Fundam. Theory Appl. **48**, 1484 (2001).

[8] Optical feedback is already a common technique in applications such as diode laser stabilization [4] and photonic signal processing [5]; it is likewise widely exploited in basic studies [6] and applications [7] of nonlinear dynamics and chaos. The present work is distinguished by its ties to recent developments in the theory of open quantum systems and quantum control. At the same time, it places new emphasis on control-theoretic concepts for the analysis of coherent optical feedback systems and illustrates the utility of the transfer-function formalism.

[9] H. M. Wiseman and G. J. Milburn, Phys. Rev. A **49**, 4110 (1994).

[10] J. F. Sherson and K. Mølmer, Phys. Rev. Lett. **97**, 143602 (2006).

[11] R. J. Nelson, Y. Weinstein, D. Cory, and S. Lloyd, Phys. Rev. Lett. **85**, 3045 (2000).

[12] The scenarios to which I refer are distinct from the coherent quantum feedback paradigm of Lloyd [11], in which a quantum controller interacts *directly* with the plant via a time-dependent Hamiltonian, without a notion of signals carried by quantum fields.

[13] M. R. James, H. I. Nurdin, and I. R. Petersen, e-print arXiv:quant-ph/0703150v2, IEEE Trans. Autom. Control (to be published).

[14] M. R. James and J. Gough, e-print arXiv:0707.1074.

[15] H. Nurdin, M. R. James, and I. R. Petersen, e-print arXiv:0711.2551.

[16] J. Gough, Commun. Math. Phys. **254**, 489 (2005).

[17] J. C. Doyle, B. A. Francis, and A. R. Tannenbaum, *Feedback Control Theory* (MacMillan, New York, 1992).

[18] H. J. Kimble, Y. Levin, A. B. Matsko, K. S. Thorne, and S. P. Vyatchanin, Phys. Rev. D **65**, 022002 (2001); T. Corbitt, N. Mavalvala, and S. Whitcomb, *ibid.* **70**, 022002 (2004).

[19] A. Ourjoumtsev, R. Tualle-Brouri, J. Laurat, and P. Grangier, Science **312**, 83 (2006); J. S. Neergaard-Nielsen, B. M. Nielsen, C. Hettich, K. Molmer, and E. S. Polzik, Phys. Rev. Lett. **97**, 083604 (2006); K. Wakui, H. Takahashi, A. Furusawa, and M. Sasaki, Opt. Express **15**, 3568 (2007).